Proinsulin Binds with High Affinity the Insulin Receptor Isoform A and Predominantly Activates the Mitogenic Pathway

Roberta Malaguarnera, Antonella Sacco, Concetta Voci, Giuseppe Pandini, Riccardo Vigneri, and Antonino Belfiore

Endocrinology (R.M., A.S., C.V., A.B.), Department of Health, University Magna Graecia of Catanzaro, 88100 Catanzaro, Italy; and Endocrinology (G.P., R.V.), Department of Clinical and Molecular Biomedicine, University of Catania, Garibaldi-Nesima Hospital, 95123 Catania, Italy

Proinsulin is generally regarded as an inactive prohormone because of its low metabolic activity. However, proinsulin appears to regulate embryo development in animal models. In this study, we evaluated whether proinsulin may differentially bind to and activate the two insulin receptor (IR) isoforms (IR-A and IR-B), because IR-A is a relatively low-specificity receptor that is prevalent in fetal and cancer cells and is able to mediate the growth effects of IGF-II. Mouse R^- fibroblasts devoid of IGF-I receptor (IGF-IR) and stably transfected with cDNA encoding either human IR-A or IR-B (R^-/IR-A and R^-/IR-B cells) were used. Three human cancer cell lines were also studied. We found that proinsulin stimulated phosphorylation of IR-A with an EC_{50} of 4.5 $\pm$ 0.6 nM and displaced [^{125}I]insulin from IR-A with a similar EC_{50}. In contrast, proinsulin EC_{50} values for stimulation of IR-B phosphorylation and for [^{125}I]insulin displacement from IR-B were approximately 7-fold higher. Proinsulin did not bind or activate IGF-IR or IR/IGF-IR hybrids. Via IR-A, proinsulin activated the ERK/p70S6K pathway to a similar degree as insulin but elicited a weaker Akt response. Despite its low metabolic activity, proinsulin was almost equipotent as insulin in inducing cell proliferation and migration in cells expressing various IR-A levels. In conclusion, proinsulin is a selective IR-A ligand and may induce biological effects through this IR isoform. (***Endocrinology*** **153: 2152–2163, 2012)**

Proinsulin is a prohormone with low metabolic activity compared with mature insulin. Proinsulin, however, may have other biological effects, as suggested by studies demonstrating roles for both insulin and proinsulin as regulators of development in prepancreatic embryonic stages (1). These studies were mostly performed in chick embryos, in which proinsulin produced before pancreas differentiation remains largely unprocessed. Proinsulin is expressed in the developing chicken retina; it plays an autocrine/paracrine stimulatory role in neurogenesis (2) and prevents cell death of neurolating embryos subjected to growth factor deprivation. In this model, excess proinsulin interferes with correct morphogenesis (1, 3). Proinsulin is also produced by the rat yolk sac in late gestational stages (4). In humans, insulin and proinsulin concentrations are significantly correlated with birth weight (5) and with various body measures including weight, length, head circumference, and skinfold thickness at birth (6). Moreover, proinsulin is biologically active in several cell types, including swine endothelial cells (7), rat intestinal stem cells (8), chick embryo fibroblasts (9), and human IM-9 lymphoblasts (10).

The receptors through which proinsulin exerts its biological effects are not fully characterized. In the chick embryo, proinsulin activates receptors that also bind insulin and IGF-I with high affinity, but these findings have not been confirmed in other cell models (1, 9).

Most studies indicate a very low metabolic activity of proinsulin and low affinity for the insulin receptor (IR) or the IGF-I receptor (IGF-IR) when evaluated in insulin target cells, such as hepatocytes and adipocytes (11, 12). Those studies, however, have never taken into account the

ISSN Print 0013-7227 ISSN Online 1945-7170
Printed in U.S.A.

doi: 10.1210/en.2011-1843 Received October 4, 2011. Accepted January 26, 2012.
First Published Online February 21, 2012

Abbreviations: BrdU, 5-bromo-2′-deoxyuridine; DG, deoxyglucose; FACS, fluorescence-activated cell sorting; FCS, fetal calf serum; FITC, fluorescein isothiocyanate; GSK, glycogen synthase kinase; IGF-IR, IGF-I receptor; IR, insulin receptor; IRS, IR substrate; T2DM, type 2 diabetes mellitus.

different functional characteristics of the two IR isoforms (IR-A and IR-B) (reviewed in Ref. 13). Indeed, the IR-A is a low-specificity receptor with high affinity not only for insulin but also for IGF-II (14), and it can also activate intracellular signaling and biological effects in response to its low-affinity ligand IGF-I (15). In contrast, IR-B is a high-specificity receptor for insulin and, during adult life, it mediates the metabolic effects of insulin in target tissues. In adult cells, IR mRNA splicing in favor of IR-B probably helps to curtail the growth effects of IGF-II through IR-A (13).

Several lines of evidence support a role for IR-A in developmental regulation in response to insulin and insulin-like peptides; for instance, transgenic mice lacking IR are growth retarded (16), and humans lacking a functioning IR also show significant growth retardation (17). These effects mainly occur via IR-A, which is predominantly expressed during prenatal life (14). IR-A, however, is also expressed in adult life, especially in cells that are not targets of the metabolic effects of insulin. In these cells, IR-A may mediate regulatory effects on growth and survival (13). IR-A is also predominant in malignant cells and appears to have a role in cancer progression and in resistance to anticancer therapies (18).

Herein we report that proinsulin binds to and activates IR-A with higher affinity than IR-B and that, by acting through the IR-A, proinsulin induces biological activities characterized by effective stimulation of cell proliferation and migration coupled with low metabolic effects. These findings may have implications in development, in insulin-resistant states and in cancer.

Materials and Methods

Reagents

The following materials were purchased: bacitracin, phenylmethylsulfonyl fluoride, porcine insulin, C-peptide, and IGF-I and IGF-II from Sigma Chemical Co. (St. Louis, MO); [^{125}I]insulin (specific activity of 81 TBq/mmol) and 2-[^{3}H]deoxyglucose (specific activity of 0.74 TBq/mmol) from PerkinElmer, Inc. (Waltham, MA); fetal calf serum (FCS) from Life Technologies, Inc. Laboratories (Paisley, UK); NVP-AEW541 from Inalco Pharmaceuticals (Milan, Italy). Human proinsulin (lot 509EM4) was provided by Lilly (Eli Lilly, Sesto Fiorentino, Italy).

Cell cultures

R^-/IR-A cells and R^-/IR-B are cell clones derived from R^- mouse embryo fibroblasts with targeted disruption of the *IGF-IR* gene; they are transfected with and express $3–5 \times 10^5$ of either IR-A (R^-/IR-A) or IR-B (R^-/IR-B) per cell. The R^+ cells are derived from R^- mouse embryo fibroblasts transfected with the human IGF-IR cDNA (14). The R^+A cells (clone A10) expressing IR/IGF-IR hybrids were obtained from R^- fibroblasts (19) by double transfection with the human cDNA for both IGF-IR and IR-A. This clone expresses $4–5 \times 10^5$ IGF-IR and $0.7–1.0 \times 10^5$ IR per cell. Under these conditions most of the IR-A hemidimers are engaged to form IR/IGF-IR hybrids. The human breast cancer cell line MDA-MB157, the human prostate cancer cells PC3, the human leiomyoarcoma cell line SKUT-1, and the rat L6 myoblasts were purchased from the American Type Culture Collection (Manassas, VA). MDA-MB157 cells were cultured in MEM with 10% FCS, PC3 cells were cultured in RPMI plus 10% FCS, and SKUT-1 cells were cultured in DMEM with 10% FCS and 1 mM Na-pyruvate. L6 myoblasts were propagated in DMEM with 25 mM glucose and 10% FCS. Differentiation was induced by switching confluent cells to differentiation medium containing 5 mM glucose and 2% FCS. Experiments were performed with fully differentiated myotubes 12–14 d after confluence.

IR phosphorylation

In vivo *studies*

Cells were stimulated with increasing doses of each ligand for 10 min or with 10 nM of each ligand for the indicated times. After cell solubilization, IR were captured by incubating cell lysates in Maxisorb plates precoated with the anti-IR antibody MA-20 (19). The immunocaptured IR were then incubated with a biotinylated antiphosphotyrosine antibody (4G10, Upstate Biotechnology, Inc., Lake Placid, NY) for 2 h at 22 C followed by peroxidase-conjugated streptavidin. The peroxidase activity was determined colorimetrically, and the absorbance was measured at 450 nm.

Studies in solubilized receptors

Unstimulated cell monolayers were solubilized, and IR were immunocaptured in Maxisorb plates coated with MA-20. Immunopurified receptors were then stimulated with increasing ligand concentrations in the presence of ATP (10 mM), $MgCl_2$ (10 mM), and $MnCl_2$ (2 mM). Plates were then washed, phosphorylated proteins were incubated with an antiphosphotyrosine biotin-conjugated antibody, and the reaction was detected as described above.

IR measurement

Cell lysates were prepared for receptor measurement by ELISA as previously described (19).

Binding studies

Binding studies were performed with intact cells that were serum starved for 16 h, washed twice with PBS, and incubated in binding buffer (14) with increasing concentrations of unlabeled ligand in the presence of radioactive [^{125}I]insulin (10 pM). After 16 h, the cell-associated radioactivity was measured in a γ-counter. Radioactivity bound in the presence of 100 nM unlabeled insulin was considered nonspecific binding.

Western blot analysis

For dose-response analysis, subconfluent cells were incubated in serum-free medium for 24 h, stimulated with increasing ligand concentrations for 10 min at 37 C, and solubilized in radioimmune

precipitation buffer. For time-course experiments, subconfluent cells were treated as above for the indicated time points.

Cell lysates were subjected to Western blot analysis (19). The antibodies used are the following: anti-IR, anti-IR substrate (IRS)1, and anti-β-tubulin (Santa Cruz Biotechnology, Inc., Santa Cruz, CA); anti-phospho(p)IR/pIGF-IR (Tyr-1150/1151), anti-pAkt(S473), anti-pAkt(T308), anti-Akt, anti-pIRS1(S636/639), anti-pIRS1(S307), anti-pIRS1(Y612), anti-pERK1/2(T202/Y204), anti-ERK1/2, anti-pp70S6K (T389), anti-p70S6K, anti-pGSK-3β (Ser9) (Cell Signaling Technology, Danvers, MA); and anti-β-actin (Sigma). Immunoblots were developed by enhanced chemiluminescence detection kit (Amersham, Little Chalfont, Buckinghamshire, UK), exposed to film, and subjected to densitometric analysis.

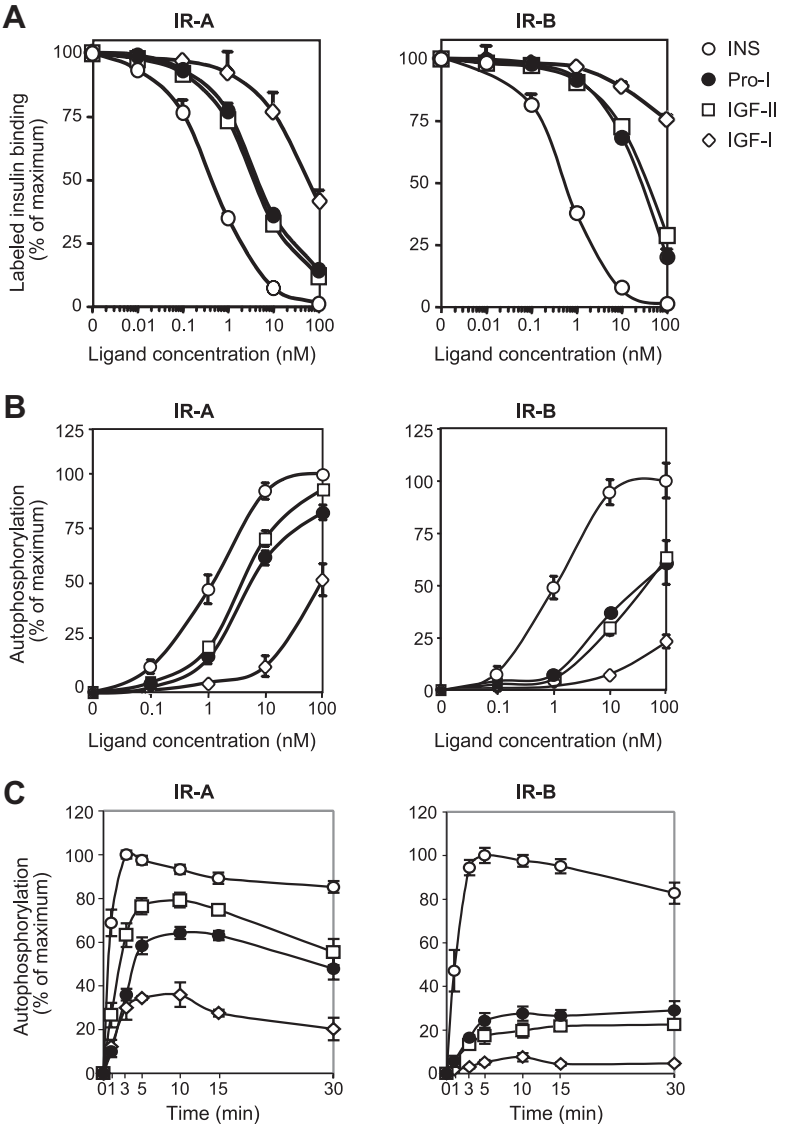

FIG. 1. Proinsulin binding and IR isoform autophosphorylation. A, Competition-inhibition curves of labeled insulin displacement from IR-A and IR-B by insulin, proinsulin, and IGFs. R⁻/IR-A (*left*) and R⁻/IR-B (*right*) cells were grown to approximately 80% confluence, serum starved for 16 h, and incubated with [^{125}I]insulin for a further 16 h at 4 C in the presence of increasing concentrations of either insulin (INS), proinsulin (Pro-I), IGF-I, or IGF-II. Cell-associated radioactivity was then measured. B and C, Dose-response and time-course studies of receptor autophosphorylation. B, R⁻/IR-A and R⁻/IR-B cells were exposed for 10 min to increasing concentrations of ligand and then solubilized. IR phosphorylation was revealed by ELISA using a specific monoclonal antibody (MA-20) to immunocapture the IR. C, Cells were exposed to 10 nM of each different ligand for different times, and IR phosphorylation was measured as described above. Data indicate mean ± SEM (*error bars*) of three to six separate experiments.

Crystal violet viability assay

Cells were seeded in 96-well plates and grown in standard cell culture medium. After serum starvation for 24 h, cells were incubated with 10 nM of ligand for 48 h. After medium removal, cells were fixed in 11% glutaraldehyde, washed in PBS, and incubated at room temperature for 20 min in staining solution (0.1% crystal violet in PBS plus 20% ethanol), washed with water, and incubated for 15 min with 10% acetic acid. The staining intensity was measured at 595 nm.

Migration assay

The ability of cells to invade Matrigel was measured with Boyden's chamber technique as described in Ref. 20. Cells, serum starved for 24 h, were placed on polycarbonate filters (8 μm pore size, Corning Costar,) coated on the upper side with 250 mg/ml collagen IV. Filters were placed over bottom chambers containing serum-free medium with or without ligand (10 nM). After incubation for 6–48 h, depending on the cell type, cells on the upper surface of filters were removed with a cotton swab, and the filters were stained for 20 min with crystal violet (0.05% crystal violet in PBS plus 20% ethanol). After three washes with water, crystal violet was solubilized in 10% acetic acid for 30 min at room temperature, and its concentration was evaluated by absorbance at 595 nm.

Proliferation assays

The incorporation of 5-bromo-2′-deoxyuridine (BrdU) during DNA synthesis in proliferating cells was measured using a nonisotopic immunoassay (DELFIA Cell Proliferation Kit, PerkinElmer). Cells were seeded in 96-well plates, serum starved for 24 h, and ligands were added for an additional 18 h. Cells were then processed according to the manufacturer's instructions. The europium fluorescence emission was measured in a time-resolved fluorometer (Wallac Victor 1420 Multilabel Counter, PerkinElmer).

For cell counts, cells were seeded in six-well plates and grown in complete medium. After serum starvation for 24 h, 10 nM of each ligand was added. After 24 and 48 h, cells were counted by trypan blue.

Cell cycle evaluation

Cells synchronized for 24 h in serum-free medium were stimulated with 10 nM ligand for 8 h (R⁻/IR-A cells) or for 48 h (all other cell types). Adherent and floating cells were harvested, resuspended in 70% ethanol, and stored at −20 C. Permeabilized cells were centrifuged and resuspended in PBS containing 20 μg/ml propidium iodide plus 40 μg/ml ribonuclease (Sigma) for 30 min. Cells

were then subjected to fluorescence-activated cell sorting (FACS) analysis (Coulter Elite flow cytometer, Beckman Coulter, Milan, Italy) and gated for DNA content (FL2) (x-axis, FL2; y-axis, events).

Apoptosis assay

Apoptosis was measured with the fluorescein isothiocyanate (FITC)-Annexin V Apoptosis Detection kit (BD Biosciences, Palo Alto, CA; PharMingen, San Diego, CA). After serum starvation for 24 h, cells were grown for 24 h in medium containing various ligands (10 nM) in the presence or the absence of different concentrations of staurosporin (2–500 nM) depending on the cell type. FITC-Annexin V-positive and propidium iodide-positive cells were evaluated according to the manufacturer's protocol and scored by FACS analysis (FITC-Annexin-V, FL1; PI, FL2).

2-[^{3}H]deoxyglucose (DG) uptake

2-[^{3}H]DG uptake was conducted in L6 myotubes. Cells were seeded in six-well plates and allowed to attach for 24 h. Complete medium was replaced with DMEM with 0.5% BSA for 4 h. After washing with 20 mM HEPES-buffered saline, cells were incubated in the same buffer for 30 min with either insulin or proinsulin at increasing concentrations. Cells were incubated for 10 min on ice with 1 μCi/ml (37 kBq/ml) 2-[^{3}H]DG (20 Ci/mmol), and 10 μM 2-DG (21). Glucose transport was terminated by removal of incubation buffer and repeated washing with PBS containing 20 mM 2-DG. Cell-associated radioactivity was measured by scintillation counting after cell solubilization with 0.03% sodium dodecyl sulfate.

IR isoform measurement

The relative abundance of IR isoforms was measured by RT-PCR as described previously (22), using primers to the flanking exons 10 and 12. After electrophoresis, the 167-bp and 131-bp DNA fragments, representing Ex11+ (IR-B isoform) and Ex11− (IR-A isoform), respectively, were analyzed by scanning densitometry. Primer sequences were forward 5′-CCAAAGACAGACTCTCAGAT-3′ and reverse 5′-AACATCGCCAAGGGACCTGC-3′.

Densitometric and statistical analysis

Densitometry results were obtained by using GelEval 1.22 software after background subtraction. Phosphorylated proteins were normalized against the nonphosphorylated counterpart. In case a signal included two bands (*e.g.* ERK1/2) both bands were measured together. Differences between means were evaluated by ANOVA (one-way or two-way when appropriate) followed by *post hoc* analysis of significance (Bonferroni test). The level of significance was set at $P < 0.05$. Statistical analysis was performed with GraphPad Prism 5 (GraphPad Software, Inc., San Diego, CA). Data are expressed as mean ± SEM (SE).

Results

Binding studies

We first evaluated the ability of proinsulin to compete with labeled insulin in cells expressing equal numbers (~3–5 × 10^5 receptors per cell) of either isoform A or isoform B of the insulin receptor (IR-A or IR-B). Competition/inhibition curves indicated that proinsulin displaced labeled insulin with an EC_{50} of 4.6 ± 1.4 nM in R^-/IR-A cells and of 28.3 ± 2.5 nM in R^-/IR-B cells. Proinsulin EC_{50} values were very similar to those of IGF-II. In contrast, IGF-I showed a much lower ability to displace labeled insulin in both cell lines, although it was more effective in R^-/IR-A cells (Fig. 1A).

Proinsulin differentially activates the two IR isoforms

Autophosphorylation of either IR-A or IR-B was evaluated by a specific ELISA in intact cells exposed to 0.1–100 nM of the different ligands for 10 min, as shown in Fig. 1B. In agreement with binding results and with previous studies (13, 14), the two IR isoforms were activated by insulin with similar high affinity, whereas IGF-II potency was approximately 28% and 3% that of insulin for IR-A and IR-B, respectively (Table 1). IGF-I was approximately 1% as potent as insulin for IR-A and even less for IR-B. Proinsulin behaved very similarly to IGF-II, with a potency approximately 20% and 3% that of insulin for IR-A and IR-B phosphorylation, respectively (Fig. 1B and Table 1). Proinsulin did not stimulate IGF-IR autophosphorylation in IGF-IR-overexpressing cells (R^+ cells) (Table 1). EC_{50} values for activation of IR isoforms and IGF-IR by the different ligands are given in Table 1.

We conducted time course experiments by stimulating cell monolayers with 10 nM of each ligand. After exposure to

TABLE 1. Autophosphorylation of IR-A, IR-B, and IGF-IR by insulin, proinsulin, IGF-II, and IGF-I

	Insulin		Proinsulin		IGF-II		IGF-I	
Cell line	EC_{50}[a]	% of activity	EC_{50}[a]	% of activity	EC_{50}[a]	% of activity	EC_{50}[b]	% of activity
R^-/IR-A	0.91 ± 0.3	100	4.5 ± 0.6	20.2	3.3 ± 0.4	27.6	80 ± 20	1.1
R^-/IR-B	1.0 ± 0.4	100	31.0 ± 6.3	3.2	36.0 ± 3.8	2.8	>100	<1
R+	>100	<1	>100	<1	2.6 ± 1.2	61.5	1.6 ± 0.4	100

For R^-/IR-A and R^-/IR-B cells the percentage of activity was calculated toward IR whereas for R+ cells the percentage of activity was calculated toward IGF-IR.

[a] EC_{50} = nM of ligand able to achieve 50% of maximal IR activation.

[b] EC_{50} = nM of ligand able to achieve 50% of maximal IGF-IR activation.

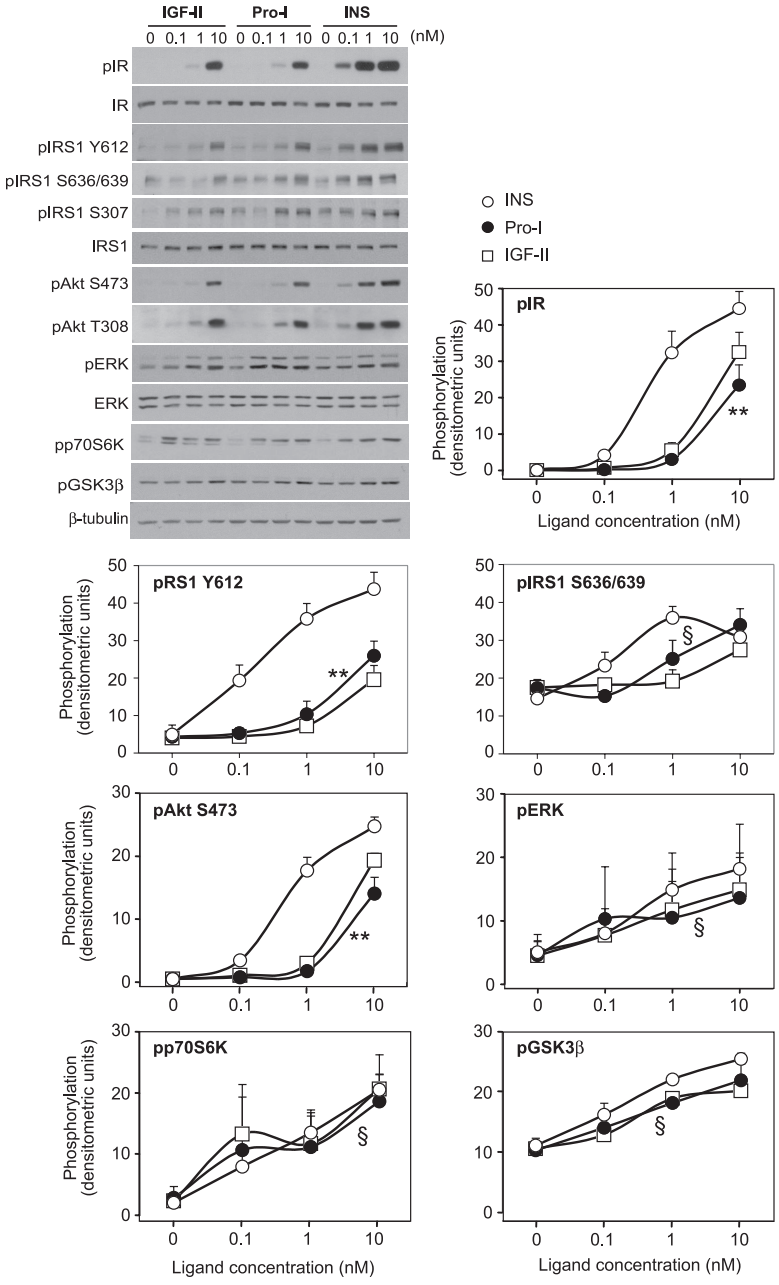

FIG. 2. Dose-response curves of IR phosphorylation and downstream signaling activation after stimulation with insulin (INS), proinsulin (pro-I), or IGF-II. R^-/IR-A cells were serum starved for 24 h, exposed for 10 min to increasing concentrations of either insulin, proinsulin or IGF-II, and then solubilized and analyzed by Western blot. Filters were probed with antibodies to the phosphorylated (p) form of pIR/pIGF-IR (Y1150/Y1151), pIRS1 (Y612, S636/639 and S307), pAkt (S473 and T308), pAkt (S473), pERK1/2 (T202/Y204), pp70S6K (T389), and pGSK3β (Ser9). Immunoblotting with anti-IR, anti-IRS1, anti-ERK1/2, and anti-β-tubulin antibodies was used to control for protein loading. The *top left panel* shows a representative experiment. *Line plots* show the mean ± SEM (*error bars*) of densitometric analyses of three separate experiments. All three ligands significantly stimulated phosphorylation at the examined phosphosites compared with unstimulated cells (at least $P < 0.05$ for all conditions). **, $P < 0.001$, stimulation curves, proinsulin *vs.* insulin; §, NS ($P > 0.05$), stimulation curves, proinsulin *vs.* insulin. For all phosphoproteins dose-response curves after proinsulin were not statistically different from those obtained after IGF-II. Statistical significance was determined using two-way ANOVA.

insulin, IR-A autophosphorylation peaked at 3–5 min and slowly decreased to approximately 80% at 30 min. IR-A autophosphorylation after proinsulin exposure was weaker ($P < 0.05$) than after insulin, and its kinetics were slightly slower, reaching a plateau between 5 and 15 min and then decreasing to approximately 75% of maximum at 30 min. Similar kinetics were observed after stimulation with IGF-II or IGF-I with a peak of IR-A phosphorylation of 80% and 35% of the maximal insulin-stimulated response, respectively (Fig. 1C, *left panel*). IR-B autophosphorylation after proinsulin stimulation reached approximately 25% of the maximal insulin-stimulated activation after 5–10 min exposure and then remained in a plateau (Fig. 1C, *right panel*). As expected, both IGF-II and IGF-I were much weaker stimulators.

Taken together, these data indicate that proinsulin differently activates the two IR isoforms (high affinity for IR-A and low affinity for IR-B), behaving similarly to IGF-II. IR-A autophosphorylation after proinsulin exposure was approximately 60–70% that for insulin but slightly delayed. IR-B autophosphorylation was much weaker ($P < 0.001$).

Autophosphorylation data in intact cells were confirmed with solubilized immunopurified receptors, which also showed that IGF-II and proinsulin had very similar EC_{50} values (see Supplemental Fig. 1A published on The Endocrine Society's Journals Online web site at http://endo.endojournals.org). Unlike exposure to proinsulin, R^-/IR-A cell exposure to 0.1–10 nM C-peptide caused no IR-A phosphorylation (Supplemental Fig. 1B). We also evaluated whether proinsulin can signal through the IGF-IR or IR-A/IGF-IR hybrid receptors. However, in R^- cells transfected with and overexpressing the human IGF-IR (R^+ cells), neither proinsulin nor insulin caused significant IGF-IR autophosphorylation (Table 1 and Supplemental Fig. 1C). Proinsulin was also unable to phosphorylate IR-A/IGF-IR hybrids that, as expected, were instead phosphorylated by IGF-I and, to a lower extent, by insulin (Supplemental Fig. 1D).

Intracellular signaling activated by proinsulin through IR-A

We evaluated the activation of key downstream kinases after R^-/IR-A cell exposure to in-

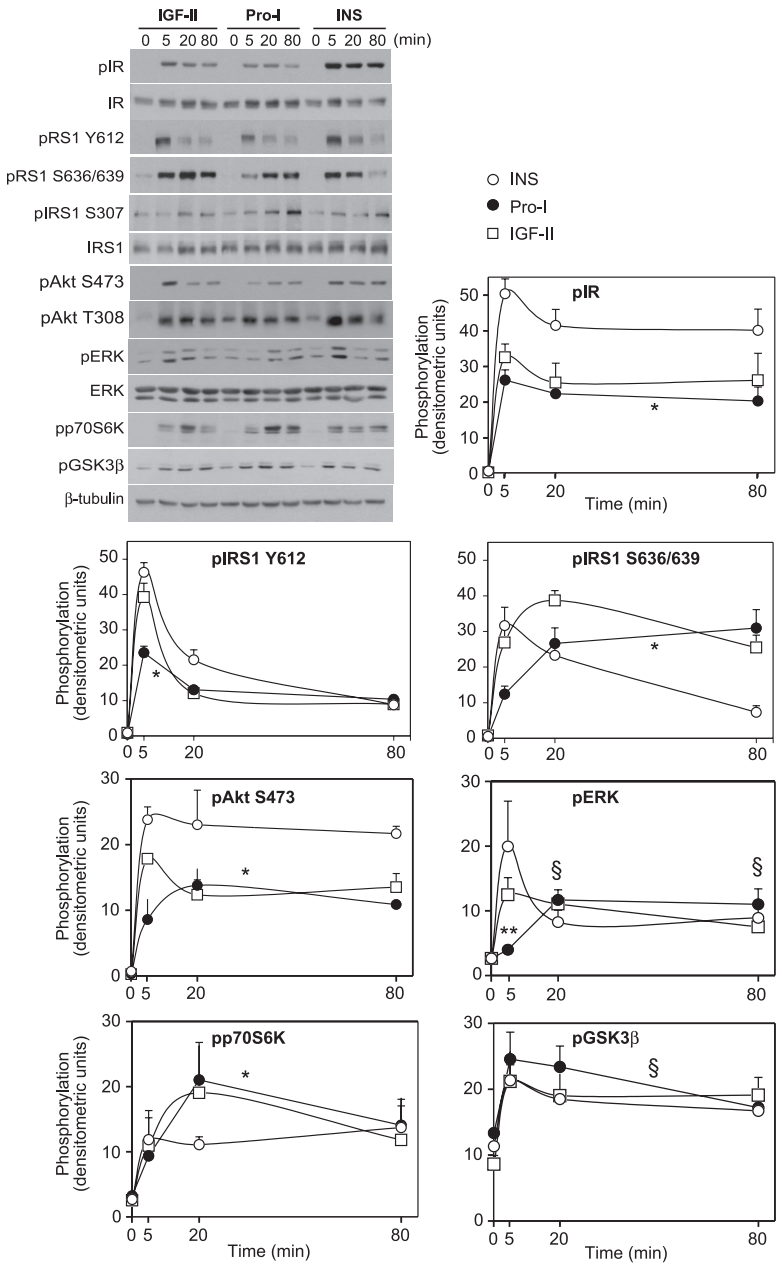

FIG. 3. Time course of IR phosphorylation and downstream signaling activation after stimulation with insulin (INS), proinsulin (pro-I), or IGF-II. R^-/IR-A cells were serum starved for 24 h and then stimulated with 10 nM of insulin, proinsulin, or IGF-II for the indicated times. Unstimulated cells are indicated as zero. Cells were then lysed and analyzed by SDS-PAGE and immunoblotting with antibodies against the phosphorylated form (p) of pIR/pIGFI-R (Y1150/Y1151), pIRS1 (Y612, S636/639 and S307), pAkt (S473 and T308), pERK1/2 (T202/Y204), pp70S6K (T389), and pGSK3β (Ser9). The *top left panel* shows a representative experiment. The same blots were probed with anti-IR, anti-IRS1, anti-ERK1/2, and anti-β-tubulin antibodies to control for protein loading. *Line plots* represent the mean ± SEM (*error bars*) of densitometric analyses of three separate experiments for IR and downstream kinases. All three ligands significantly stimulated phosphorylation at these phosphosites compared with unstimulated cells (at least $P < 0.05$ for all conditions). *, $P < 0.05$, stimulation curves, proinsulin *vs.* insulin; **, $P < 0.01$, proinsulin *vs.* insulin (pp70S6K, 5 min); §, NS ($P > 0.05$), stimulation curve, proinsulin *vs.* insulin (pGSK3β); and proinsulin *vs.* insulin (pp70S6K, 20 min and 80 min). For all phosphoproteins time course curves after proinsulin and after IGF-II were not statistically different. Statistical significance was determined using two-way ANOVA.

creasing doses of either insulin or proinsulin, or IGF-II, for 10 min. Western blot analysis, in accordance with ELISA studies, indicated that IR-A autophosphorylation was much weaker with proinsulin and IGF-II than with insulin ($P < 0.001$). IRS1 tyrosine phosphorylation (Tyr612) and Akt phosphorylation (both at Ser473 and Thr308) followed a pattern similar to that of receptor autophosphorylation, with insulin being a stronger stimulator than proinsulin and IGF-II ($P < 0.001$) (Fig. 2). In contrast, despite a lower phosphorylation of the receptor, both proinsulin and IGF-II stimulated the phosphorylation of ERK1/2, glycogen synthase kinase (GSK)3β, and p70S6K to a similar level than insulin (Fig. 2). When the phosphorylation of Akt (Ser475) and ERK1/2 was normalized for the amount of IR activation, it appeared that 0.1 and 1 nM proinsulin induced a much higher ERK1/2 activation for amount of phosphorylated IR-A, compared with insulin (Supplemental Fig. 2).

Time course experiments, performed by Western blot, confirmed data obtained by ELISA on IR-A autophosphorylation (Fig. 1C, *left panel*), indicating that proinsulin was approximately 2-fold less effective than insulin ($P < 0.05$) (Fig. 3). IRS1 tyrosine phosphorylation (Tyr612) and Akt phosphorylation (at Ser475 and Thr308) followed a similar pattern, with lower values ($P < 0.05$) after proinsulin than after insulin exposure. Proinsulin also caused weaker ERK1/2 phosphorylation than insulin or IGF-II at 5 min ($P < 0.001$) but induced sustained phosphorylation from 20–80 min, similarly to insulin and IGF-II (NS) (Fig. 3). The phosphorylation time course of GSK3β and p70S6K was similar (NS) for the three ligands (Fig. 3).

As readout of downstream kinases activity, we evaluated the phosphorylation of IRS1 at Ser-636/Ser-639 and Ser-307. These serines are phosphorylated by p70S6K/mammalian target of rapamycin, c-Jun N-terminal kinase, and other kinases after IR ligand stimulation (23–25). Overall, the degree of IRS1 serine phosphorylation after proinsulin was not significantly different from that reached after insulin (Fig. 2), in agreement with the high p70S6K activation observed after proinsulin. However, IRS1 Ser-636/Ser-639 phosphorylation occurred at early time points in response to insulin, whereas it was delayed in response to proinsulin (Fig. 3).

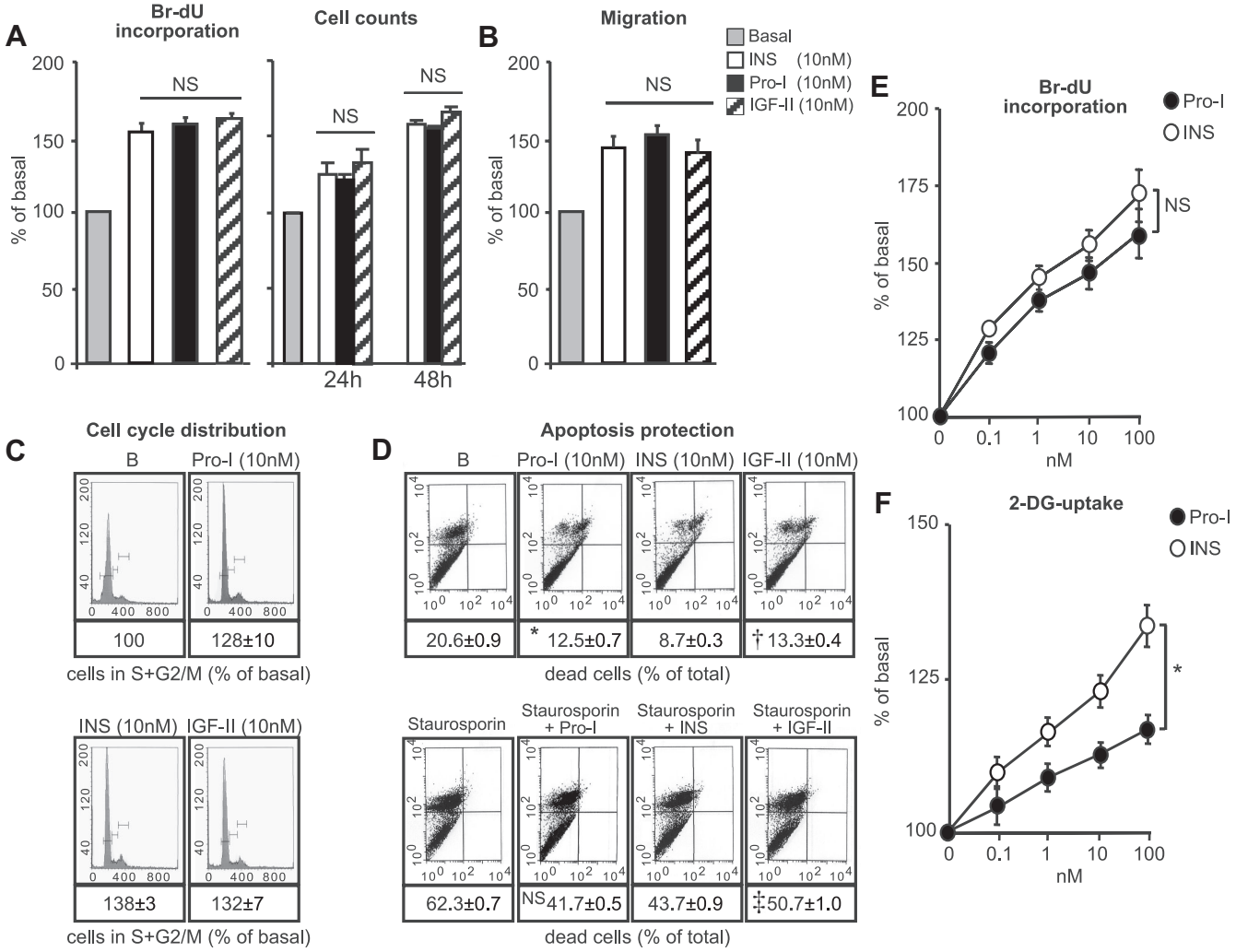

FIG. 4. Mitogenic and metabolic effects induced by proinsulin (pro-I) in R⁻/IR-A cells. A, BrdU incorporation and cell counts. BrdU incorporation (*left panel*): R⁻/IR-A cells were serum starved for 24 h and then exposed to 10 nM of either proinsulin or insulin (INS) for a further 18 h. BrdU was then added, and the cells were incubated for 2 h at 37 C. The percentage of BrdU-labeled nuclei was then measured. Cell counts (*right panel*): R⁻/IR-A cells were serum starved for 24 h and then exposed to 10 nM of either proinsulin or insulin. After 24 h or 48 h of treatment, cells were collected by trypsinization and counted. Values are expressed as percentages of untreated cells (indicated as B) and are the mean ± SEM (*error bars*) of three separate experiments performed in triplicate. NS ($P > 0.05$): not statistically significant (proinsulin *vs.* insulin and IGF-II *vs.* insulin, using one-way ANOVA followed by Bonferroni test). B, Cell migration. Migration experiments were conducted by evaluating the ability of R⁻/IR-A cells to invade Matrigel using the Boyden's chamber technique. Cells were allowed to migrate in the lower side of collagen-coated transwells for 6 h in the absence (basal) or the presence of 10 nM proinsulin, insulin, or IGF-II. Values are expressed as percentages of basal (B). NS ($P > 0.05$), Not statistically significant (proinsulin *vs.* insulin, using one-way ANOVA followed by Bonferroni test). C, Cell cycle progression. R⁻/IR-A cells were serum starved for 24 h and then exposed to 10 nM of either proinsulin, insulin, or IGF-II for 8 h. Cell cycle distribution was evaluated by propidium iodide staining and FACS analysis. Panels show the cell cycle profile of untreated (B) and stimulated cells of a representative experiment. *Below* each cell cycle profile the percentage of cells in S and G_2/M phases is indicated. Values are expressed as percent of basal and are the mean ± SEM (*error bars*) of three separate experiments. There is no significant difference ($P > 0.05$) among the three ligands (one-way ANOVA followed by Bonferroni test). D, Apoptosis protection. Serum-starved R⁻/IR-A cells were exposed to 10 nM proinsulin, insulin, or IGF-II in presence or absence of staurosporin (2 nM) for 24 h. Cells were then stained with both FITC-Annexin V and propidium iodide and subjected to FACS analysis. A representative experiment is shown. Values *below* each flow cytometric analysis plot indicate the total number of dead cells, including those in early apoptosis (FITC Annexin-V positive and propidium iodine negative) and those in end-stage apoptosis or already dead (stained by both FITC Annexin-V and propidium iodine). Values are expressed as percent of total scored cells and are the mean ± SEM (*error bars*) of three separate experiments. NS ($P > 0.05$); *, $P < 0.05$; †, $P < 0.005$; ‡, $P < 0.0005$, compared with insulin (one-way ANOVA followed by Bonferroni test). E, Dose-response cell proliferation experiments. Serum-starved R⁻/IRA cells were grown in 96-well plates and then exposed to either proinsulin or insulin at the indicated concentrations for 48 h. Cell viability was then tested by BrdU incorporation. Values are expressed as percentages of untreated cells and are the mean ± SEM (*error bars*) of three separate experiments performed in triplicate. NS ($P > 0.05$), Proinsulin compared with insulin (two-way ANOVA followed by Bonferroni test). F, 2-DG uptake. L6 myotubes were incubated with insulin or proinsulin at the indicated concentrations for 30 min in HEPES-buffered saline solution. Next, ^{3}H-labeled 2-DG (1 μCi/ml) was added for 10 min, and the uptake was measured. Values are expressed as percent of maximum and represent the mean ± SEM (*error bars*) of three independent experiments. NS ($P > 0.05$), *, $P < 0.05$, dose-response curve after proinsulin *vs.* after insulin (two-way ANOVA followed by Bonferroni test).

Prolonged insulin incubation induces degradation of both IR and IRS1, a phenomenon that may contribute to fine tuning of intracellular signaling. We observed that degradation of both IR and IRS1 after proinsulin exposure was delayed compared with insulin exposure (Supplemental Fig. 3A).

To confirm that these intracellular effects of proinsulin were truly dependent on IR-A autophosphorylation, we measured in parallel experiments IR-A phosphorylation in response to proinsulin (1–10 nM) after cell preincubation with the IR/IGF-IR tyrosine kinase inhibitor NVP-AEW541 (3 μM). Under these conditions both Akt phosphorylation and ERK1/2 phosphorylation were strongly inhibited, indicating that these effects were indeed dependent on IR-A autophosphorylation (Supplemental Fig. 3B). Given the stronger receptor activation by insulin, inhibition of insulin-dependent signaling was less marked.

Taken together, these data indicate that in R$^-$/IR-A cells, despite inducing lower IR-A phosphorylation, proinsulin activates intracellular signaling pathways that (compared with insulin-activated signaling) are characterized by sustained ERK1/2 activation and an increased ERK1/2-Akt activation ratio at later time points. Moreover, proinsulin is able to stimulate GSK3β phosphorylation similarly to insulin and to activate p70S6K at similar or even higher levels than insulin. In general, intracellular signaling via IR-A followed a similar pattern after exposure to proinsulin or IGF-II.

Proinsulin induces biological effects through the IR-A

We then measured various biological effects in cells exposed to either proinsulin, insulin, or IGF-II. R$^-$/IR-A cells were used for evaluating proliferation, cell cycle progression, protection from apoptosis and migration, whereas L6 myotubes were used for evaluating 2-DG uptake.

At 10 nM, all three ligands elicited a similar proliferative response, as assessed by BrdU incorporation and direct cell counts (Fig. 4A) and crystal violet staining (data not shown). Similar results were observed with chemoinvasion (Fig. 4B) and cell cycle progression (Fig. 4C). Both proinsulin and IGF-II were slightly less potent than insulin for protecting cells from serum starvation-induced apoptosis. However, proinsulin was equally potent than insulin for staurosporin-induced apoptosis protection with IGF-II being slightly less effective (Fig. 4D).

Dose-response experiments indicated that proinsulin stimulates BrdU incorporation in a dose-dependent manner, with a significant effect at concentrations as low as 0.1 nM and with a pattern similar to that of insulin (at 100 nM, the proinsulin effect was 83.0 ± 1.3% that of insulin; NS, proinsulin *vs.* insulin) (Fig. 4E). In contrast, proinsulin at the highest dose was significantly less effective than insulin in stimulating 2-DG uptake in L6 myotubes ($P < 0.05$) (Fig. 4F). At 100 nM, proinsulin induced only approximately 55% of the maximal 2-DG uptake obtained with insulin. Proinsulin therefore elicits relevant biological effects via IR-A, with mitogenic and migratory activity comparable to that induced by insulin.

TABLE 2. IR content and IR-A isoform relative abundance in SKUT-1, MDA-MB157, and PC3 cells

	IR content	
	IR (ng/100 μg protein)	% IR-A
SKUT-1	4.3 ± 0.8	94%
MDA-MB157	5.2 ± 0.9	70%
PC3	9.5 ± 2.2	65%

IR total content was measured by ELISA, and the % IR-A was calculated after IR isoform measurement by RT-PCR, as described in *Materials and Methods*.

Studies in human cancer cell lines

We then studied proinsulin effects in three human cancer cell lines, SKUT-1, MDA-MB157, and PC3, which are characterized by various expression levels of IR-A and different IR-A:IR-B ratios (Table 2).

In all three cell lines, the activation of IR was significantly lower after proinsulin than after insulin treatment (Fig. 5), whereas the degree of ERK1/2 phosphorylation was similar (NS) with the two ligands (Fig. 5). Other downstream kinases had a more variable response in the different cell lines. In PC3 cells, proinsulin and insulin were equipotent for the activation of all downstream kinases. In SKUT-1 cells, proinsulin induced levels of p70S6K and GSK3β phosphorylation similar to insulin but lower Akt activation. In MDA-MB157 cells proinsulin elicited a weaker activation response than insulin for Akt, p70S6K, and GSK3β (Fig. 5).

The biological responses to 10 nM proinsulin or insulin were then evaluated. As shown in Fig. 6, in SKUT-1 and PC3 cells, the two ligands were similarly effective except for stimulation of migration, in which proinsulin was weaker. In MDA-MB157 cells, proinsulin was slightly but significantly less effective for all examined effects (except for cell cycle progression).

Dose-response experiments showed that proinsulin, starting at 0.1 nM, stimulates BrdU incorporation in a dose-dependent manner, with a potency that in SKUT-1 and MDA-MB157 cells was slightly but significantly lower than that of insulin, whereas in PC3 cells was similar to that of insulin except at the highest dose. At 100 nM, in all three cell lines, proinsulin elicited approximately 80% of the insulin response (Supplemental Fig. 4). Parallel ex-

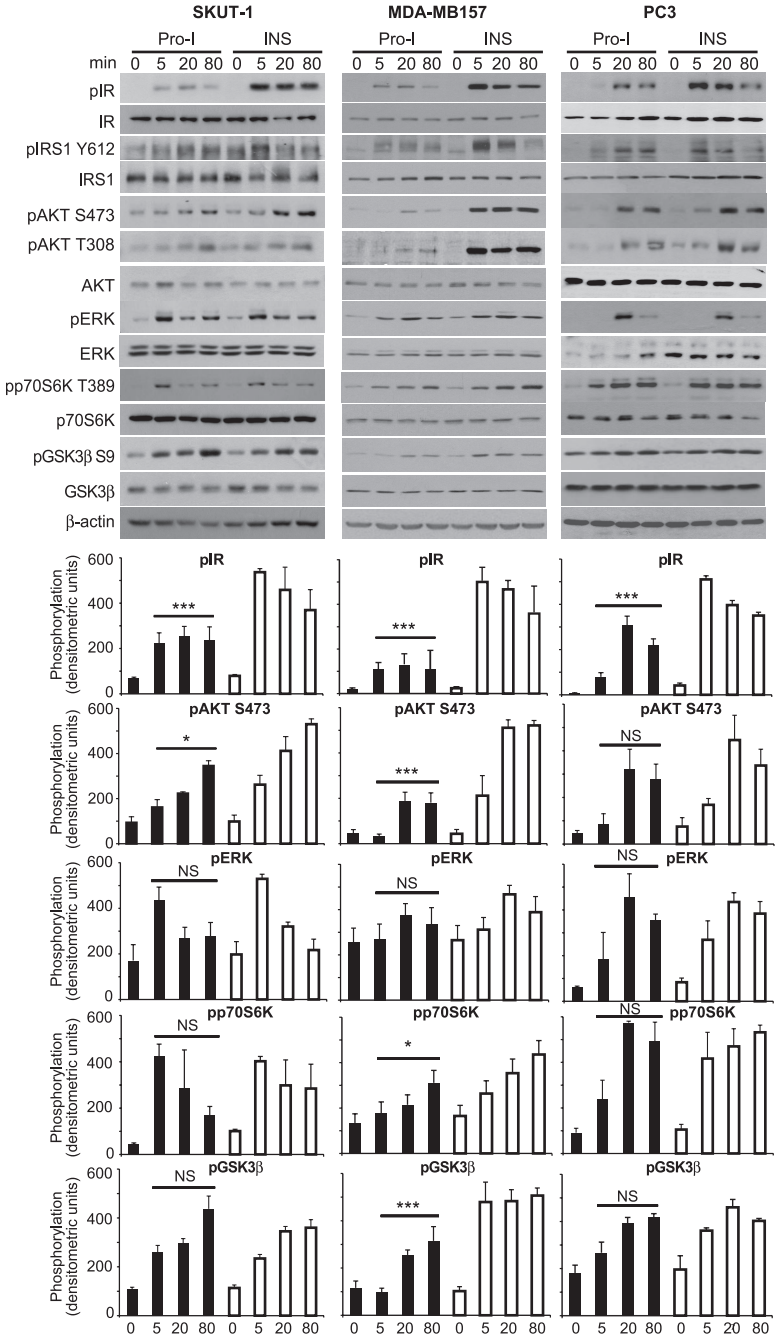

FIG. 5. Intracellular signaling pattern induced by proinsulin (pro-I) in human cancer cell lines. The human cancer cell lines SKUT-1, MDA-MB157, and PC3 were serum starved for 24 h and then stimulated with 10 nM proinsulin or insulin (INS) for the indicated times. Cells were lysed, analyzed by SDS-PAGE, and immunoblotted with antibodies against the phosphorylated form (p) of pIR/pIGF-IR (Y1150/Y1151), pAkt (S473), pAkt (T308), pERK1/2 (T202/Y204), pp70S6K (T389), and pGSK3β (Ser9). The same blots were probed with anti-IR, anti-Akt, anti-ERK1/2, anti-p70S6K, anti-GSK3β, and anti-β-actin antibodies to control for protein loading. The *top panels* show, for each cell line, a representative experiment. The *histograms* represent the mean ± SEM (*error bars*) of densitometric analyses of three separate experiments after normalization of each phosphopeptide against the total, nonphosphorylated form. Statistical significance was determined using two-way ANOVA. *, $P < 0.05$; **, $P < 0.01$, ***, $P < 0.001$ (proinsulin *vs.* insulin stimulation curve). NS, Not statistically significant ($P > 0.05$).

periments with crystal violet staining provided similar results (data not shown).

In line with what we observed in R^+ cells, proinsulin was unable to stimulate IGF-IR phosphorylation in human cancer cells (Supplemental Fig. 5). Because these cancer cells also contain IR/IGF-IR hybrids, we evaluated whether IR/IGF-IR could be implicated in the response to proinsulin. After cell incubation with proinsulin, anti-pY immunoprecipitates contained only IR and not IGF-IR moieties, indicating that IR/IGF-IR hybrids were not stimulated by proinsulin (Supplemental Fig. 5).

Discussion

Proinsulin is currently regarded as a prohormone with low affinity for the IR (11, 12) and little biological activity. Our present results show that proinsulin differentially binds to and activates the two IR isoforms, with a higher affinity for IR-A than for IR-B. This behavior is remarkably similar to that of IGF-II (13, 14), although, at variance with IGF-II, proinsulin has no activity toward the IGF-IR or IR/IGF-IR hybrids. In R^-/IR-A cells (expressing only IR-A and lacking both IGF-IR and IR-B), proinsulin consistently activated downstream signaling pathways with a different pattern compared with insulin. In particular, proinsulin stimulated p70S6K activation to a similar or greater extent than insulin, while being approximately 2- to 3-fold less potent than insulin for Akt activation at 10 nM (Fig. 3). This pattern of intracellular signaling is also shared by IGF-II (15). Moreover, IRS1 Ser636/639 phosphorylation, a mechanism involved in signaling termination (26, 27), was delayed after proinsulin compared with insulin. Finally, degradation of IR and IRS1 occurred only after 24 h of continuous stimulation with proinsulin whereas it was clearly evident after 8 h of insulin stimulation. This delayed degradation response, possibly related to the low binding affinity of proinsulin to the IR-A, may result in a longer ligand-receptor interaction. All these factors may contribute to the increased mitogenic-metabolic ratio observed with proinsulin or IGF-II compared with insulin (15). Our present data are in agreement with findings describing nonparallel metabolic and growth-promoting effects of various types of insulin (28).

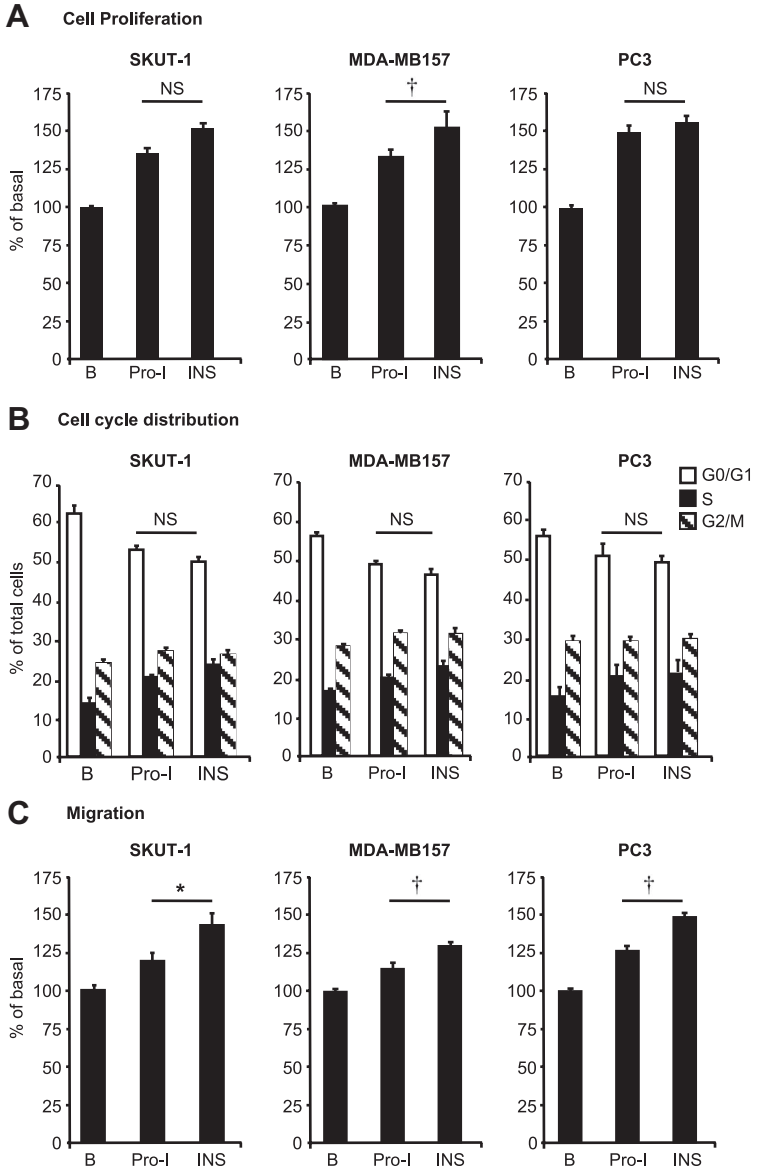

FIG. 6. Biological effects of proinsulin (pro-I) in human cancer cell lines. A, Cell proliferation. SKUT-1, MDA-MB157, and PC3 human cancer cells were grown in 96-well plates, serum starved for 24 h, and then exposed to 10 nM of either proinsulin or insulin for a further 48 h. Cell viability was evaluated by crystal violet staining. Values are expressed as percentages of untreated cells (indicated as b) and are the mean ± SEM (*error bars*) of three separate experiments performed in triplicate. NS ($P > 0.05$), *, $P < 0.05$, proinsulin *vs.* insulin (one-way ANOVA followed by Bonferroni test). B, Cell cycle analysis. Cancer cells, after serum starvation for 24 h, were analyzed for their cell-cycle profiles before and after treatment with 10 nM proinsulin or insulin for 48 h. Cell populations positive for PI staining were evaluated by FACS analysis, and G_0/G_1, S, and G_2/M phases were scored. *White columns,* Cells in G_0/G_1; *black columns,* cells in S; *hatched columns*, cells in G_2/M. Each column indicates the percentage of total cells (mean of three separate experiments done in triplicate). NS ($P > 0.05$), for G_0/G_1 in proinsulin *vs.* insulin-treated cells (one-way ANOVA followed by Bonferroni test). C, Cell migration. Subconfluent SKUT-1, MDA-MB157, and PC3 cells, after serum starvation for 24 h, were seeded on polycarbonate filters in the presence or the absence of 10 nM ligand. Cells that migrated to the lower compartment were measured after 6 h (MDA-MB-157) or 48 h (SKUT-1 and PC3). Values [mean ± SEM (*error bars*) of three separate experiments done in triplicate] are expressed as percent of untreated cells (B). *, $P < 0.05$; †, $P < 0.005$, proinsulin *vs.* insulin (one-way ANOVA followed by Bonferroni test).

In three different human cancer cell lines, predominantly expressing the IR-A isoform, downstream signaling in response to proinsulin was variable, although ERK1/2 was always similarly stimulated by proinsulin and insulin. In SKUT-1 cells, only Akt had a weaker response to proinsulin compared with insulin, whereas in MDA-MB157 cells the responses of Akt, p70S6K, and GSK3β were weaker after proinsulin. In PC3 cells proinsulin and insulin were equipotent for the stimulation of all downstream kinases studied. In all three cancer cell lines, IR autophosphorylation was substantially weaker after proinsulin than after insulin.

Proinsulin elicited an effective stimulation of cell proliferation and migration. In PC3 cells, the cells with the highest absolute IR-A content, signaling, and growth differences between proinsulin and insulin were the smallest. It is worth noting that IR-A/IR-B hybrid receptors, which are functionally similar to IR-A (29), may affect proinsulin response, whereas IR/IGF-IR hybrids are unresponsive to proinsulin.

Our data may contribute to a better knowledge of IR isoform physiology, which is still incompletely understood (13, 30). During the early stages of development proinsulin is secreted by chick retinal cells, where it promotes cell proliferation, differentiation, and survival (1). The importance of IR, which in the chick is expressed exclusively as IR-A, is underlined by the finding that IR silencing induces retinal cells apoptosis (31). Moreover, transgenic mice with specific inactivation of the *IR* gene in rod photoreceptors show retinal degeneration, providing strong evidence for a role of IR in photoreceptor cell function and survival. These findings have been confirmed in rats in which IR activity is independent of mature insulin, leaving open the possibility that IR is instead activated by proinsulin (32). By identifying IR-A as a proinsulin receptor, our present findings may provide new impetus for future studies in this field.

In humans, the proinsulin-insulin concentration ratio has been reported to be approximately 6-fold higher in newborns than in adults (6), suggesting that proinsulin may elicit biological effects in prenatal/early neonatal life, in accordance with the role of the insulin/

IGF pathway in the biology of progenitor/stem cells (33–37).

Whether proinsulin may also elicit biological effects in adult life is unknown. In normal adults, proinsulin is present in the bloodstream at concentrations less than 10 pM, whereas it reaches levels of 10–50 pM or higher in insulin-resistant type 2 diabetes mellitus (T2DM) patients (38), who also have an increased proinsulin-insulin ratio (39). In T2DM patients, proinsulin levels are associated with carotid intima-media wall thickness, a marker for atherosclerosis and cardiovascular disease (40). Proinsulin-insulin ratio increases with age (41), and in elderly men high proinsulin levels are predictive of stroke, whereas insulin levels are not (42). Proinsulin levels are also associated with increased activity of the plasminogen activator inhibitor-1, the main regulator of fibrinolysis (7), and levels greater than 45 pM are considered a marker of high cardiovascular risk (43). Moreover, administration of exogenous biosynthetic proinsulin to T2DM patients is associated with an increased incidence of cardiovascular events (44). In our *in vitro* model, proinsulin starts eliciting biological activities in cultured cells at picomolar concentrations, and it could be hypothesized that elevated proinsulin levels may affect the development or progression of malignancies that overexpress IR-A (14, 22, 45). It is noteworthy that T2DM and obese patients show up to 2- to 3-fold increased risk for various malignancies (46, 47) and poor cancer prognosis (48). More studies are needed to verify these possibilities.

In summary, proinsulin by acting as a selective IR-A ligand may stimulate cell proliferation and migration to a similar degree as insulin. In view of these characteristics, proinsulin may play a biological role via IR-A activation during development and in insulin-resistant individuals.

Acknowledgments

We thank Eli Lilly (Italy) for the gift of human proinsulin. We thank Dr. Francesco Frasca (Department of Clinical and Molecular Biomedicine, University of Catania) for useful discussion.

Address all correspondence and requests for reprints to: Antonino Belfiore, Department of Health, Endocrinology, University of Catanzaro, Campus Universitario, località Germaneto, 88100 Catanzaro, Italy. E-mail: belfiore@unicz.it.

This work was supported by grants from the Associazione Italiana per la Ricerca sul Cancro (AIRC) to A.B. (grant n. 10625) and R.V., and AIRC project Calabria 2011 and Fondazione Cassa di Risparmio di Calabria e Lucania (to A.B.), and from PRIN-MIUR, grant 2008BKRFBH_005, (to A.B.).

Disclosure Summary: The authors have nothing to disclose.

References

1. **Hernández-Sánchez C, Mansilla A, de la Rosa EJ, de Pablo F** 2006 Proinsulin in development: new roles for an ancient prohormone. Diabetologia 49:1142–1150
2. **Hernández-Sánchez C, López-Carranza A, Alarcón C, de La Rosa EJ, de Pablo F** 1995 Autocrine/paracrine role of insulin-related growth factors in neurogenesis: local expression and effects on cell proliferation and differentiation in retina. Proc Natl Acad Sci USA 92:9834–9838
3. **Hernández-Sánchez C, Rubio E, Serna J, de la Rosa EJ, de Pablo F** 2002 Unprocessed proinsulin promotes cell survival during neurulation in the chick embryo. Diabetes 51:770–777
4. **Muglia L, Locker J** 1984 Extrapancreatic insulin gene expression in the fetal rat. Proc Natl Acad Sci USA 81:3635–3639
5. **Dornhorst A, Nicholls JS, Ali K, Andres C, Adamson DL, Kelly LF, Niththyananthan R, Beard RW, Gray IP** 1994 Fetal proinsulin and birth weight. Diabet Med 11:177–181
6. **Shields BM, Knight B, Hopper H, Hill A, Powell RJ, Hattersley AT, Clark PM** 2007 Measurement of cord insulin and insulin-related peptides suggests that girls are more insulin resistant than boys at birth. Diabetes Care 30:2661–2666
7. **Schneider DJ, Nordt TK, Sobel BE** 1992 Stimulation by proinsulin of expression of plasminogen activator inhibitor type-I in endothelial cells. Diabetes 41:890–895
8. **Jehle PM, Fussgaenger RD, Angelus NK, Jungwirth RJ, Saile B, Lutz MP** 1999 Proinsulin stimulates growth of small intestinal crypt-like cells acting via specific receptors. Am J Physiol 276:E262–E268
9. **Morales AV, Serna J, Alarcón C, de la Rosa EJ, de Pablo F** 1997 Role of prepancreatic (pro)insulin and the insulin receptor in prevention of embryonic apoptosis. Endocrinology 138:3967–3975
10. **Jehle PM, Lutz MP, Fussgaenger RD** 1996 High affinity binding sites for proinsulin in human IM-9 lymphoblasts. Diabetologia 39:421–432
11. **Burguera B, Frank BH, DiMarchi R, Long S, Caro JF** 1991 The interaction of proinsulin with the insulin-like growth factor-I receptor in human liver, muscle, and adipose tissue. J Clin Endocrinol Metab 72:1238–1241
12. **Podlecki DA, Frank BH, Olefsky JM** 1984 In vitro characterization of biosynthetic human proinsulin. Diabetes 33:111–118
13. **Belfiore A, Frasca F, Pandini G, Sciacca L, Vigneri R** 2009 Insulin receptor isoforms and insulin receptor/insulin-like growth factor receptor hybrids in physiology and disease. Endocr Rev 30:586–623
14. **Frasca F, Pandini G, Scalia P, Sciacca L, Mineo R, Costantino A, Goldfine ID, Belfiore A, Vigneri R** 1999 Insulin receptor isoform A, a newly recognized, high-affinity insulin-like growth factor II receptor in fetal and cancer cells. Mol Cell Biol 19:3278–3288
15. **Sacco A, Morcavallo A, Pandini G, Vigneri R, Belfiore A** 2009 Differential signaling activation by insulin and insulin-like growth factors I and II upon binding to insulin receptor isoform A. Endocrinology 150:3594–3602
16. **Louvi A, Accili D, Efstratiadis A** 1997 Growth-promoting interaction of IGF-II with the insulin receptor during mouse embryonic development. Dev Biol 189:33–48
17. **Jospe N, Kaplowitz PB, Furlanetto RW** 1996 Homozygous nonsense mutation in the insulin receptor gene of a patient with severe congenital insulin resistance: leprechaunism and the role of the insulin-like growth factor receptor. Clin Endocrinol (Oxf) 45:229–235
18. **Belfiore A** 2007 The role of insulin receptor isoforms and hybrid insulin/IGF-I receptors in human cancer. Curr Pharm Des 13:671–686
19. **Pandini G, Frasca F, Mineo R, Sciacca L, Vigneri R, Belfiore A** 2002 Insulin/insulin-like growth factor I hybrid receptors have different biological characteristics depending on the insulin receptor isoform involved. J Biol Chem 277:39684–39695

20. **Sieg DJ, Ilić D, Jones KC, Damsky CH, Hunter T, Schlaepfer DD** 1998 Pyk2 and Src-family protein-tyrosine kinases compensate for the loss of FAK in fibronectin-stimulated signaling events but Pyk2 does not fully function to enhance FAK-cell migration. EMBO J 17:5933–5947
21. **Sweeney G, Somwar R, Ramlal T, Volchuk A, Ueyama A, Klip A** 1999 An inhibitor of p38 mitogen-activated protein kinase prevents insulin-stimulated glucose transport but not glucose transporter translocation in 3T3–L1 adipocytes and L6 myotubes. J Biol Chem 274:10071–10078
22. **Vella V, Pandini G, Sciacca L, Mineo R, Vigneri R, Pezzino V, Belfiore A** 2002 A novel autocrine loop involving IGF-II and the insulin receptor isoform-A stimulates growth of thyroid cancer. J Clin Endocrinol Metab 87:245–254
23. **Tremblay F, Gagnon A, Veilleux A, Sorisky A, Marette A** 2005 Activation of the mammalian target of rapamycin pathway acutely inhibits insulin signaling to Akt and glucose transport in 3T3–L1 and human adipocytes. Endocrinology 146:1328–1337
24. **Aguirre V, Werner ED, Giraud J, Lee YH, Shoelson SE, White MF** 2002 Phosphorylation of Ser307 in insulin receptor substrate-1 blocks interactions with the insulin receptor and inhibits insulin action. J Biol Chem 277:1531–1537
25. **Zick Y** 2005 Ser/Thr phosphorylation of IRS proteins: a molecular basis for insulin resistance. Sci STKE 2005:pe4
26. **Shah OJ, Hunter T** 2006 Turnover of the active fraction of IRS1 involves raptor-mTOR- and S6K1-dependent serine phosphorylation in cell culture models of tuberous sclerosis. Mol Cell Biol 26: 6425–6434
27. **Tzatsos A, Kandror KV** 2006 Nutrients suppress phosphatidylinositol 3-kinase/Akt signaling via raptor-dependent mTOR-mediated insulin receptor substrate 1 phosphorylation. Mol Cell Biol 26: 63–76
28. **King GL, Kahn CR** 1981 Non-parallel evolution of metabolic and growth-promoting functions of insulin. Nature 292:644–646
29. **Blanquart C, Achi J, Issad T** 2008 Characterization of IRA/IRB hybrid insulin receptors using bioluminescence resonance energy transfer. Biochem Pharmacol 76:873–883
30. **Moller DE, Yokota A, Caro JF, Flier JS** 1989 Tissue-specific expression of two alternatively spliced insulin receptor mRNAs in man. Mol Endocrinol 3:1263–1269
31. **Díaz B, Serna J, De Pablo F, de la Rosa EJ** 2000 In vivo regulation of cell death by embryonic (pro)insulin and the insulin receptor during early retinal neurogenesis. Development 127:1641–1649
32. **Rajala A, Tanito M, Le YZ, Kahn CR, Rajala RV** 2008 Loss of neuroprotective survival signal in mice lacking insulin receptor gene in rod photoreceptor cells. J Biol Chem 283:19781–19792
33. **Stachelscheid H, Ibrahim H, Koch L, Schmitz A, Tscharntke M, Wunderlich FT, Scott J, Michels C, Wickenhauser C, Haase I, Brüning JC, Niessen CM** 2008 Epidermal insulin/IGF-1 signalling control interfollicular morphogenesis and proliferative potential through Rac activation. EMBO J 27:2091–2101
34. **Yan YP, Sailor KA, Vemuganti R, Dempsey RJ** 2006 Insulin-like growth factor-1 is an endogenous mediator of focal ischemia-induced neural progenitor proliferation. Eur J Neurosci 24:45–54
35. **McDevitt TC, Laflamme MA, Murry CE** 2005 Proliferation of cardiomyocytes derived from human embryonic stem cells is mediated via the IGF/PI 3-kinase/Akt signaling pathway. J Mol Cell Cardiol 39:865–873
36. **Dallas NA, Xia L, Fan F, Gray MJ, Gaur P, van Buren II G, Samuel S, Kim MP, Lim SJ, Ellis LM** 2009 Chemoresistant colorectal cancer cells, the cancer stem cell phenotype, and increased sensitivity to insulin-like growth factor-I receptor inhibition. Cancer Res 69: 1951–1957
37. **Malaguarnera R, Frasca F, Garozzo A, Giani F, Pandini G, Vella V, Vigneri R, Belfiore A** 2011 Insulin receptor isoforms and insulin-like growth factor receptor in human follicular cell precursors from papillary thyroid cancer and normal thyroid. J Clin Endocrinol Metab 96:766–774
38. **Pfützner A, Kunt T, Hohberg C, Mondok A, Pahler S, Konrad T, Lübben G, Forst T** 2004 Fasting intact proinsulin is a highly specific predictor of insulin resistance in type 2 diabetes. Diabetes Care 27: 682–687
39. **Festa A, Williams K, Hanley AJ, Haffner SM** 2008 Beta-cell dysfunction in subjects with impaired glucose tolerance and early type 2 diabetes: comparison of surrogate markers with first-phase insulin secretion from an intravenous glucose tolerance test. Diabetes 57: 1638–1644
40. **Haffner SM, D'Agostino R, Mykkänen L, Hales CN, Savage PJ, Bergman RN, O'Leary D, Rewers M, Selby J, Tracy R, Saad MF** 1998 Proinsulin and insulin concentrations in relation to carotid wall thickness: Insulin Resistance Atherosclerosis Study. Stroke 29: 1498–1503
41. **Bryhni B, Arnesen E, Jenssen TG** 2010 Associations of age with serum insulin, proinsulin and the proinsulin-to-insulin ratio: a cross-sectional study. BMC Endocr Disord 10:21
42. **Wiberg B, Sundström J, Zethelius B, Lind L** 2009 Insulin sensitivity measured by the euglycaemic insulin clamp and proinsulin levels as predictors of stroke in elderly men. Diabetologia 52:90–96
43. **Pfützner A, Kann PH, Pfützner AH, Kunt T, Larbig M, Weber MM, Forst T** 2004 Intact and total proinsulin: new aspects for diagnosis and treatment of type 2 diabetes mellitus and insulin resistance. Clin Lab 50:567–573
44. **Galloway JA, Hooper SA, Spradlin CT, Howey DC, Frank BH, Bowsher RR, Anderson JH** 1992 Biosynthetic human proinsulin. Review of chemistry, in vitro and in vivo receptor binding, animal and human pharmacology studies, and clinical trial experience. Diabetes Care 15:666–692
45. **Sciacca L, Mineo R, Pandini G, Murabito A, Vigneri R, Belfiore A** 2002 In IGF-I receptor-deficient leiomyosarcoma cells autocrine IGF-II induces cell invasion and protection from apoptosis via the insulin receptor isoform A. Oncogene 21:8240–8250
46. **Vigneri P, Frasca F, Sciacca L, Pandini G, Vigneri R** 2009 Diabetes and cancer. Endocr Relat Cancer 16:1103–1123
47. **Pisani P** 2008 Hyper-insulinaemia and cancer, meta-analyses of epidemiological studies. Arch Physiol Biochem 114:63–70
48. **Calle EE, Rodriguez C, Walker-Thurmond K, Thun MJ** 2003 Overweight, obesity, and mortality from cancer in a prospectively studied cohort of U.S. adults. N Engl J Med 348:1625–1638